Mesenchymal stem cell therapy promotes renal repair by limiting glomerular podocyte and progenitor cell dysfunction in adriamycin-induced nephropathy

Carla Zoja, Pablo Bautista Garcia, Cinzia Rota, Sara Conti, Elena Gagliardini, Daniela Corna, Cristina Zanchi, Paolo Bigini, Ariela Benigni, Giuseppe Remuzzi and Marina Morigi

Mesenchymal stem cell therapy promotes renal repair by limiting glomerular podocyte and progenitor cell dysfunction in adriamycin-induced nephropathy

Carla Zoja,[1] Pablo Bautista Garcia,[1] Cinzia Rota,[1] Sara Conti,[1] Elena Gagliardini,[1] Daniela Corna,[1] Cristina Zanchi,[1] Paolo Bigini,[2] Ariela Benigni,[1] Giuseppe Remuzzi,[1,3] and Marina Morigi[1]

[1]*Mario Negri Institute for Pharmacological Research, Centro Anna Maria Astori, Science and Technology Park Kilometro Rosso, Bergamo, Italy;* [2]*Department of Biochemistry and Molecular Pharmacology, Mario Negri Institute for Pharmacological Research, Milano, Italy; and* [3]*Unit of Nephrology and Dialysis, Azienda Ospedaliera Ospedali Riuniti di Bergamo, Bergamo, Italy*

Zoja C, Garcia PB, Rota C, Conti S, Gagliardini E, Corna D, Zanchi C, Bigini P, Benigni A, Remuzzi G, Morigi M. Mesenchymal stem cell therapy promotes renal repair by limiting glomerular podocyte and progenitor cell dysfunction in adriamycin-induced nephropathy. *Am J Physiol Renal Physiol* 303: F1370–F1381, 2012. First published September 5, 2012; doi:10.1152/ajprenal.00057.2012.—We previously reported that in a model of spontaneously progressive glomerular injury with early podocyte loss, abnormal migration, and proliferation of glomerular parietal epithelial progenitor cells contributed to the formation of synechiae and crescentic lesions. Here we first investigated whether a similar sequence of events could be extended to rats with adriamycin (ADR)-induced nephropathy. As a second aim, the regenerative potential of therapy with bone marrow-derived mesenchymal stem cells (MSCs) on glomerular resident cells was evaluated. In ADR-treated rats, decrease of $WT1^+$ podocyte number due to apoptosis was associated with reduced glomerular expression of nephrin and CD2AP. As a consequence of podocyte injury, glomerular adhesions of the capillary tuft to the Bowman's capsule were observed, followed by crescent-like lesions and glomerulosclerosis. Cellular components of synechiae were either $NCAM^+$ parietal progenitor cells or $nestin^+$ podocytes. In ADR rats, repeated injections of MSCs limited podocyte loss and apoptosis and partially preserved nephrin and CD2AP. MSCs attenuated the formation of glomerular podocyte-parietal epithelial cell bridges and normalized the distribution of $NCAM^+$ progenitor cells along the Bowman's capsule, thereby reducing glomerulosclerosis. Finding that MSCs increased glomerular VEGF expression and limited microvascular rarefaction may explain the prosurvival effect by stem cell therapy. MSCs also displayed anti-inflammatory activity. Coculture of MSCs with ADR-damaged podocytes showed a functional role of stem cell-derived VEGF on prosurvival pathways. These data suggest that MSCs by virtue of their tropism for damaged kidney and ability to provide a local prosurvival environment may represent a useful strategy to preserve podocyte viability and reduce glomerular inflammation and sclerosis.

mesenchymal stem cells; podocytes; parietal epithelial progenitor cells; renal repair; adriamycin nephropathy; vascular endothelial growth factor

CHRONIC KIDNEY DISEASES (CKD) are emerging as a global threat to public health, with an estimated prevalence of 11% of the adult population in Western industrialized nations (17). CKD requiring renal replacement therapy, i.e., dialysis or renal transplantation, are rising sharply. Renal transplantation is limited by organ shortage, and in the next decade, the cost for dialysis will become unbearable even in the most developed countries (22). Although considerable gains have been obtained in retarding progression of CKD by renin-angiotensin system blockade in a significant proportion of patients, the therapeutic goal of arresting CKD progression to end-stage renal disease remains unfulfilled.

The kidney has been classically considered as an organ with minimal cellular turnover and low capacity for regeneration. The identification of renal stem/progenitor cells has challenged this view. Cellular therapies or regenerative treatment for the injured kidney targeting progenitors represent an innovative strategy. A population of glomerular progenitor cells localized along the Bowman's capsule with the potential to regenerate podocytes has been described in humans (39, 40). Clinical and experimental evidence indicates that depending on the cause and associated environmental factors, damage and loss of podocytes are critical determinants in the progression of glomerular diseases to hyperplastic and/or sclerotic lesions (44, 45). In a rat model of spontaneously progressive glomerulopathy, we (3) recently documented an aberrant migration and proliferation of glomerular parietal progenitor cells, reflecting dysregulation of their ability to restore lost podocytes, that contributed to crescent formation and glomerulosclerosis. In this model, the ACE inhibitor by moderating progenitor cell activation restored glomerular architecture and limited renal disease progression. On the other hand, stem cell-based therapy exploiting the stem cell peculiar properties of renal tropism and regenerative capability may also contribute to kidney repair. Bone marrow-derived mesenchymal stem cells (MSCs), or stromal cells, are a source of multipotent cells having the potential of tissue regeneration in experimental models of myocardial infarction (24, 33, 47), neurological disease (51), and acute kidney injury (19, 21, 30, 31). We showed that infusion of murine (21, 30) and human MSCs (31) in mice with acute kidney injury decreased renal tubular injury and ameliorated renal function impairment, which translated into reduced animal mortality. The mechanism underlying renoprotection and renal repair was ascribed to local production of regenerative and prosurvival factors including insulin-like growth factor-1 by MSCs (21), rather than their differentiation into renal cells. In rat models of ischemia/reperfusion injury, MSCs released at the site of their engraftment, factors with antiapoptotic, anti-inflammatory and angiogenic properties (49, 50). Among these, vascular endothelial growth factor (VEGF) was recognized as an important mediator of MSC-induced renoprotection to the extent that silencing of VEGF by small-interfering RNA reduced effectiveness of MSC and decreased survival in rats with acute kidney injury (48).

1931-857X/12 Copyright © 2012 the American Physiological Society

The therapeutic potential of MSCs in animal models of chronic nephropathies has not been completely established so far. MSC treatment improved interstitial fibrosis and loss of peritubular capillaries, but it failed to prevent the progression of CKD in mice with Alport disease (34). Infusion of MSCs in rats with 5/6 nephrectomy partially preserved renal function and attenuated glomerulosclerosis (7) and interstitial fibrosis (41). Early treatment with MSCs blunted glomerulosclerosis in an adriamycin (ADR) model of nephropathy, while it failed to modify proteinuria and progression of renal failure (28).

In the present study, we first investigated in the rat model of ADR-induced nephropathy, whether glomerular podocyte injury was associated with dysfunction of glomerular parietal epithelial progenitor cells, as recently documented in a model of spontaneous glomerulopathy (3). We then evaluated if treatment of nephrotic rats with ex vivo expanded bone marrow-derived MSCs, a cell source of prosurvival and angiogenic factors, had regenerative effects on cells of distinct glomerular compartments as podocytes, parietal epithelial cells (PECs), and endothelial cells.

MATERIALS AND METHODS

Isolation of Rat MSCs

MSCs were obtained from bone marrow of 2-mo-old male Lewis rats (Charles River), as previously described (13). Briefly, bone marrow was flushed from the shaft of the bone and filtered through a 100-μm sterile filter (BD Biosciences, Milan, Italy). Filtered bone marrow cells were plated in α-MEM (Invitrogen, Paisley, Scotland) plus 20% FCS (Invitrogen) and penicillin-streptomycin (100 U/ml to 0.1 mg/ml; Invitrogen) and allowed to adhere for 24 h. After 2 to 3 wk, subconfluent cells were detached by trypsin-EDTA (0.5 to 0.2 g/l; Invitrogen). The MSC preparation used for the in vivo experiments derived from a pool of MSCs obtained by bone marrow collected from 12 Lewis rats. FACS analysis revealed that MSCs were negative (98% negative cells) for the hematopoietic marker CD45 (anti rat-CD45 Ab, BD Pharmingen). MSCs were characterized for their capability to differentiate toward adipocytes and osteocytes as shown in Fig. 1, A and B.

Adipogenesis. MSCs were incubated for 3 wk with 5 μg/ml insulin, 10^{-6} M dexamethasone, 0.5 μM isobutylmethylxanthine, and 50 μM indomethacin. Then, cells were fixed with 10% formalin, and oil red O staining was used to visualize the accumulation of lipid droplets into the cell vacuoles (Fig. 1A).

Osteogenesis. Cultures were fed twice a week for 3 wk with 10 mM β-glycero-phosphate, 0.2 mM ascorbic acid 2-phosphate, and 10^{-8} M dexamethasone. Then, the cells were fixed and extensive mineralization of the extracellular matrix was visualized by alizarin red S (all reagents were from Sigma-Aldrich, St Louis, MO; Fig. 1B).

Rat Model of ADR-Induced Nephropathy

Male Lewis rats (Charles River Laboratories Italia, Calco, Italy), with initial body weights of 200–250 g, were used. Animal care and treatment were in accordance with institutional guidelines in compliance with national (D.L. n.116, G.U., suppl 40, 18 February 1992, Circolare No. 8, G.U., 14 July 1994) and international laws and policies (EEC Council Directive 86/609, OJL 358, Dec 1987; NIH Guide for the Care and Use of Laboratory Animals, U.S. National Research Council, 1996). Animal studies were submitted to and approved by the Institutional Animal Care and Use Committee of "Mario Negri" Institute (Milan, Italy). Animals were housed in a constant temperature room with a 12:12-h dark-light cycle and fed a standard diet. Disease was induced by a single dose of ADR (5 mg/kg; Pfeizer Italia, Latina, Italy) by tail-vein infusion. ADR-treated rats were intravenously injected with saline ($n = 16$) or MSCs (2×10^6 cells; $n = 16$) derived from bone marrow of male Lewis rats, at different times after ADR, i.e., 36 and 60 h and 3, 5, 7, 14, and 21 days, to ensure the presence of MSCs in the kidney during time. Before injection, MSCs were labeled with PKH-26 red fluorescence cell linker (Sigma-Aldrich). In selected experiments, ADR-treated rats ($n = 3$) were injected with MSCs labeled with polymeric large nanoparticles (fluoNP). Labeled MSCs were washed twice with saline and resuspended in saline for the injection in ADR-treated rats. Six normal rats intravenously injected with saline served as controls. Twenty-four-hour urine samples were collected using metabolic cages, and proteinuria was determined by the Coomassie protein assay (Sigma Aldrich). Serum creatinine was measured by the Reflotron test (Roche Diagnostics, Indianapolis, IN). Rats were killed at 3, 9, 16, and 30 days after ADR, and kidneys were removed for histology and immunohistochemistry analysis.

Identification of Labeled MSCs

To study intrarenal localization, rat MSCs were labeled with PKH-26 red fluorescence cell linker (Sigma-Aldrich) before injection into ADR-treated rats. Labeling efficiency was assessed to be >98%. Viability evaluated by Trypan blue exclusion was >96%. Rats were killed at different times, and kidney samples were fixed in paraformaldehyde-lysine-periodate and sections stained with FITC-labeled lectin wheat germ agglutinin (WGA; Vector Laboratories, Burlingame, CA) and DAPI (Sigma-Aldrich). Slides were analyzed for PKH-26-positive cells. A number of nine sections per rat ($n = 3$ rats) were analyzed, and PKH-26-positive cells were counted. Data were expressed as number of PKH-26-positive cells/100,000 renal cells. In
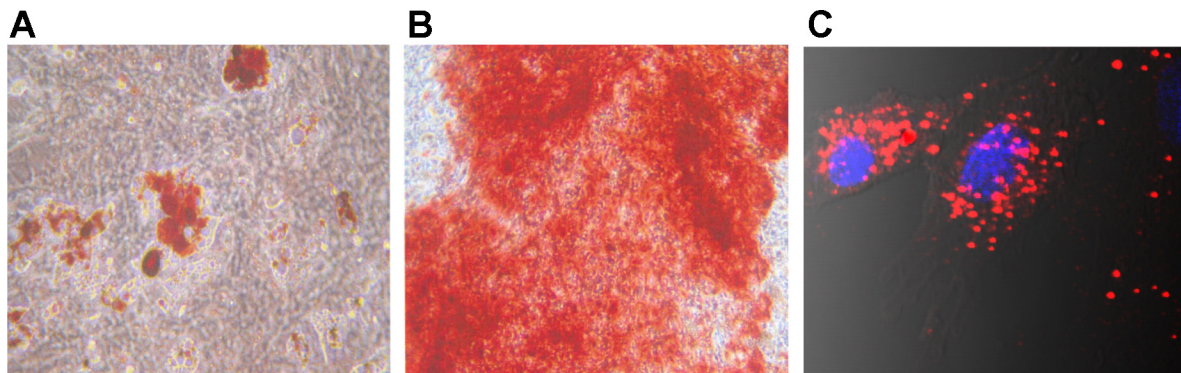
Fig. 1. *A*: representative micrograph of rat mesenchymal stem cells (MSCs) showing differentiation into adipocytes as visualized by intracellular lipid vacuoles detected with oil Red O staining. *B*: differentiation toward osteocytes is indicated by the formation of calcium-rich hydroxyapatite detected with alizarin red. *C*: representative image of fluo-NP-labeled MSCs (red) costained with Hoechst 33258 for cell nuclei (blue). Original magnification: ×400.

addition, we evaluated the presence of MSCs into the damaged kidney by tracking MSCs with polymeric 200-nm large nanoparticles (fluoNP, kindly provided by Dr. Davide Moscatelli, Politecnico di Milano, Italy) in which the dye rhodamine-B was covalently bounded to the polymer to avoid the risk of leakage of the fluorescent compound once injected in animals. Briefly, MSCs were incubated for 72 h with polymeric nanoparticles (35 μg/ml). At the end of the incubation, MSCs were resuspended in sterile saline and injected into the tail vein of ADR-treated rats ($n = 3$). To verify the efficiency of the labeling, a small aliquot of MSCs was fixed with 4% paraformaldehyde in PBS, costained with Hoechst 33258, and visualized with an Olympus Fluoview microscope BX61 with confocal system FV500 (Fig. 1C). FACS analysis was used to quantify the number of fluoNP-labeled MSCs in the kidneys of ADR-treated rats killed at 3 days. Briefly, kidneys were minced and digested with collagenase IV (300 U/ml; Worthington Biochemical, Lakewood, NJ) for 45 min at 37°C. The cell suspension was filtered through a 100-μm sterile filter and washed with PBS, and red emission for nanoparticles was analyzed by using BD FACSCanto II (BD Biosciences). Kidneys isolated from ADR-treated rats that did not receive fluoNP-labeled MSCs were used as negative control.

Renal Morphology

Kidney samples were fixed in Duboscq-Brazil. Paraffin-embedded sections (3-μm) were stained with periodic acid-Schiff reagent. At least 15–20 glomeruli were examined for each rat, and the extent of synechiae was expressed by giving a score from 0 to 4 related on the percentage of glomerular tuft occupied by the lesions (0: no lesions; 1: lesions affecting <25% of the glomerulus; 2: lesions affecting >25 to 50% of the glomerulus; 3: lesions affecting >50 to 75% of the glomerulus; and 4: lesions affecting >75 to 100% of the glomerulus). Data are expressed as percentage of glomeruli with different degree of lesions (synechiae and more extensive adhesions). To evaluate the extent of glomerular sclerosis, an average of 35 glomeruli was examined and data were expressed as glomerular sclerosis index. Each glomerulus was scored according to the extension of sclerotic changes as follows: 0 = absence of sclerosis; 1 = sclerotic changes affecting <25% of glomerular tuft area; 2 and 3 = lesions affecting >25 to 50% and >50 to 75% of the tuft; and 4 = lesions exceeding 75% of the tuft. The average glomerulosclerosis index in each animal was then calculated by the weight-average of each class (10). All renal biopsies were analyzed by the same pathologist who was unaware of the nature of the experimental groups.

Immunohistochemistry

For immunofluorescence experiments, sections (3-μm) from paraformaldehyde-lysine-periodate-fixed kidney specimens were analyzed. After antigen unmasking and blocking of nonspecific sites, sections were incubated with the following primary antibodies: rabbit anti-Wilm's tumor 1 (WT1; 2 μg/ml in PBS, Santa Cruz Biotechnology, Santa Cruz, CA), goat anti-nephrin (0.2 μg/ml in PBS; Santa Cruz), rabbit anti-CD2AP (0.2 μg/ml in PBS; Santa Cruz), rabbit anti-claudin1 (undiluted, Thermo Scientific, Rockford, IL), mouse anti-nestin (1:100; BD Biosciences), mouse anti-NCAM (1:2, Developmental Studies Hybridoma Bank, University of Iowa), and mouse anti-rat endothelial cell antigen (RECA-1; 1:100, R&D Systems, Oxon, UK). Then, the sections were incubated with the appropriate secondary antibodies (Jackson Immunoresearch). Slides were counterstained with DAPI (Sigma-Aldrich), and those incubated with anti-WT-1 antibodies were counterstained with FITC-labeled WGA (Vector Laboratories). Some sections were coincubated with anti-WT1 and anti-nestin antibodies. Double and triple fluorescence labeling were analyzed by an inverted confocal laser scanning microscope (LS 510 Meta; Zeiss, Jena, Germany), and 30 random images for each sample were acquired. Glomerular expression of the podocyte-associated proteins nephrin, CD2AP, and nestin was estimated by calcu-

lating the proportion of area occupied by the staining within each glomerulus, using NIH ImageJ software and a Mac OS PC (Apple computer, Cupertino, CA). At least 30 randomly chosen glomeruli per section were analyzed. To evaluate whether MSCs acquired a podocyte phenotype, in some experiments kidney sections from ADR-treated rats injected with PKH-26-labeled MSCs (*day 16*) were stained with anti-WT1 antibody followed by Cy5-donkey anti rabbit antibody (Jackson Immunoresearch).

A mouse monoclonal antibody (1:100; Chemicon, Temecula, CA) was used for the detection of monocyte/macrophage ED-1 surface antigen by alkaline phosphatase-Fast Red technique on paraffin-embedded sections (55). ED-1-positive cells were counted in at least 30 randomly selected glomeruli (×400) per each animal.

Immunoperoxidase method (4) was employed for detection of VEGF using goat anti-VEGF antibody (1:10; R&D Systems) that detects rat $VEGF_{164}$. Intensity of glomerular VEGF signal was graded on a scale of 0 to 3 (0, no staining; 1, weak staining, 2; staining of moderate intensity; and 3, strong staining). Negative controls were obtained by omitting the primary antibody on adjacent sections (data not shown).

Morphometrical Analysis

Glomerular podocytes were identified as cells positive for WT1. Estimation of glomerular volume was performed using a computer-based image analysis system (Mac OS09; Apple Computer) as previously described (27). Mean value of glomerular volume and the estimation of the average number of podocytes per glomerulus were determined by the stereological method of particle density proposed by Weibel (53).

Volume density of glomerular endothelial cells was estimated as area density occupied by RECA-1 staining. Twenty renal sections per rat were digitalized using an inverted confocal laser microscopy (original magnification, ×630; LSM 510 Meta; Carl Zeiss, Jena, Germany). Each image (512 × 512 pixels) was digitally overlapped with an orthogonal grid composed of 2,500 points (ImageJ; NIH, Bethesda, MD). The volume density of endothelial cells was calculated as the ratio of the number of grid points hitting RECA-1 staining to the total number of grid points falling into the total area occupied by the glomerulus.

Apoptosis

Apoptosis was detected by enzymatic labeling of DNA strand breaks using a terminal deoxynucleotidyl transferase-mediated deoxyuridine triphosphate nick end-labeling (TUNEL) assay (Roche Diagnostics). Nuclei were labeled by DAPI. Podocytes were identified by WT-1 staining, as described above. Triple fluorescence labeling was analyzed by an inverted confocal laser scanning microscope (LSM 510 Meta; Carl Zeiss), and 30 random images for each sample were acquired.

Western Blot Analysis

Frozen kidney tissues were homogenized in lysis buffer (50 mM Tris·HCl pH 8, 150 mM NaCl, 1% Triton X-100, 0.5% sodium deoxycholate, and 0.1% SDS) containing the Halt protease inhibitor cocktail (Thermo Scientific, Rockford, IL). Protein concentration was determined using the bicinchoninic acid assay (Thermo Scientific) following the manufacturer's instructions. The samples (50 μg) were resolved on 7–15% SDS-polyacrylamide gel and transferred to nitrocellulose membrane. After blocking, membranes were incubated 4°C overnight with anti-$VEGF_{164}$ antibody (1:200; R&D Systems) or anti-α-tubulin antibody (1:4,000; Sigma-Aldrich) and with an appropriate secondary antibody (Sigma-Aldrich). Protein bands were detected by supersignal chemiluminescent substrate (GE Healthcare) and quantified using NIH ImageJ software. The amount of VEGF protein was calculated relative to the level of α-tubulin.

In Vitro Experiments

Immortalized mouse podocytes (obtained from Dr. Peter Mundel, Dept. of Medicine, Mount Sinai School of Medicine, New York, NY) were grown and differentiated as described (32). Murine MSCs were obtained from bone marrow of 2-mo-old male C57BL6/J mice as previously reported (30). Cells were plated and grown in DMEM plus 10% FCS and penicillin-streptomycin (100 U/ml to 0.1 mg/ml). After 2 to 3 wk, subconfluent (80%−90%) cells were detached by trypsin-EDTA (0.5 to 0.2 g/l; Invitrogen) and immunodepleted of CD45-positive cells (30). For coculture experiments, podocytes were seeded at 23×10^3 cells/cm^2 and 14 days later were incubated with RPMI (Invitrogen) plus 10% FCS (test medium) alone or in the presence of 1.5 μM ADR (Pfeizer) for 6 h. After drug withdrawal, podocytes were incubated with test medium or with MSCs at the density of 23×10^3 cells/cm^2 (1:1) for 72 h, and then total viable cells were counted by trypan blue dye exclusion (Sigma-Aldrich). The number of adherent podocytes was obtained by counting total viable cells in coculture subtracted of MSC number. The percentage of viable podocytes in each sample was calculated vs. control podocytes imposed as 100%. The role of VEGF was studied by adding to ADR-treated podocytes cocultured with MSCs, functional blocking anti-VEGF antibody (10 μg/ml; R&D Systems) for 72 h. In additional samples, exogenous recombinant mouse VEGF-A (40 ng/ml; Immunotools, Germany) was added to podocytes treated with ADR. It was previously shown that differentiated murine podocytes express VEGF receptors (16, 18, 46).

Apoptosis Assay

Apoptosis was assessed by studying the expression of cytocrome *c* at 3, 15, and 24 h after ADR incubation in cultured cells fixed with 2% paraformaldehyde and 4% sucrose for 10 min. Cells were permeabilized, incubated with blocking solution, and then with anti-cytochrome *c* antibody (1:100; BD Bioscience) followed by secondary antibody (FITC goat anti-mouse IgG). Nuclei were counterstained with DAPI. Apoptotic podocytes are expressed as percentage of cells with cytocrome *c* in the cell cytosol per total cells.

Apoptosis was also evaluated by assessment of cleaved caspase-3 at 3 and 15 h after ADR incubation. Cells were permeabilized and incubated with blocking solution and then with anti-cleaved caspase-3 antibody (1:400; Cell Signaling, MA) followed by an appropriate secondary antibody (FITC donkey anti-rabbit IgG). Cells were analyzed by FACS at 488 nm excitation, green emission for cleaved caspase-3. Data are expressed as percentage of apoptotic cells.

Western Blot Analysis

The expression of Akt and pAkt was studied in control podocytes exposed to medium, in ADR-treated podocytes incubated with medium, exogenous VEGF-A (40 ng/ml), or with MSC-conditioned medium (24-h conditioned medium) for 72 h. Podocytes were lysed with lysis buffer (20 mM Tris·HCl pH 7.5, 1% Triton X-100, 25 mM NaCl, 1.5 mM EDTA, 50 mM NaF, and 15 mM Na$_4$P$_2$O$_7$) containing protease inhibitor (Complete, Roche Diagnostic). Protein lysates were separated on 10% polyacrylamide gel by SDS-PAGE (Bio-Rad, Milan, Italy) and transferred to nitrocellulose membrane. After blocking, membranes were incubated overnight with primary antibodies against Akt or p-Akt Ser473 (1:1,000; Cell Signaling Technology, Danvers, MA) and with an appropriate secondary antibody (Sigma-Aldrich). Protein bands were detected by supersignal chemiluminescent substrate (GE Healthcare, UK).

Statistical Analysis

Results are expressed as means ± SE. Data were analyzed by nonparametric Mann-Whitney test or Kruskal-Wallis test for multiple comparisons followed by Ryan's procedure or by ANOVA test coupled with Bonferroni post hoc analysis, as appropriate. The statistical significance level was defined as $P < 0.05$.

RESULTS

In Vivo Studies

Glomerular changes in rats with ADR nephropathy. Glomerular podocytes are target of injury in a variety of kidney diseases (42, 54), and reduction of podocyte number is followed by glomerular parietal epithelial progenitor cell migration and proliferation to regenerate lost cells (25). Here, we characterized changes occurring in podocytes and PECs in rats with ADR nephropathy during time. To determine whether podocyte number was reduced following ADR treatment, triple labeling of glomeruli with WT1, a podocyte-specific marker that localizes in nuclei of podocytes appearing red, fluorescein-WGA (lectin) that stains the glomerular capillaries, and DAPI that stains all cell nuclei was performed. Superimposed images of WT1 and DAPI showed less pink staining of podocyte nuclei in glomeruli of ADR-treated animals compared with glomeruli from control rats (Fig. 2A). By morphometric analysis, a significant decrease in the number of WT1-positive cells was observed after ADR injection, starting from 3 days, with respect to control rats (ADR, *day 3*: 129.57 ± 3.56; *day 9*: 127.01 ± 2.83; *day 16*: 122.84 ± 5.37 vs. control, 221.99 ± 5.66 podocytes/glomerulus; $P < 0.01$). Podocyte loss in response to ADR was confirmed by immunostaining with nestin, a specific marker of podocytes (glomerular area percentage: ADR, *day 3*: 10.25 ± 4.16% vs. control, 16.00 ± 0.75%; $P < 0.01$). Loss of podocytes in ADR-treated rats was coupled to slit diaphragm protein alterations, as documented by reduced and discontinuous staining of nephrin (Fig. 2B), which functions to maintain slit pore integrity and renal filtration capacity (52) (glomerular area percentage: ADR, *day 9*: 1.69 ± 0.05 vs. control 10.84 ± 0.41%; $P < 0.05$), and by decreased expression of CD2AP (Fig. 2C) a protein associated to nephrin (43) (glomerular area percentage: ADR, *day 9*: 2.85 ± 0.43 vs. control, 15.06 ± 0.23%; $P < 0.05$).

Given the reduction in podocyte number in response to ADR administration, the TUNEL assay was next performed to establish whether apoptosis could account for podocyte depletion in these animals. A high number of apoptotic podocytes, as identified by double-staining for TUNEL and WT1, was detected in the renal tissue of ADR rats given saline, at variance with kidneys from control rats where no apoptotic podocytes were detected (ADR, *day 3*: 17.8 ± 0.54; *day 9*: 16.79 ± 0.78; *day 16*: 15.34 ± 0.61 vs. control, 0 TUNEL/WT1-positive podocytes/glomerulus).

As a consequence of ADR-induced podocyte injury, glomerular adhesions of the capillary tuft to the Bowman's capsule (synechiae) were observed starting from 16 days and were followed by crescents-like lesions at 30 days (Fig. 3A). The phenotype of cells contributing to early lesions of ADR-treated rats was then assessed by studying the expression of claudin1, an intercellular tight junction protein constitutively expressed by all glomerular PECs lining the Bowman's capsule (35) (Fig. 3B) and of nestin, a marker of podocytes (38). Costaining of claudin1 and nestin revealed that PECs and podocytes both participated to the formation of early cellular bridges at 16 days (Fig. 3B). At the same time, parietal progenitor cells expressing the metanephric mesenchymal marker NCAM (1, 2, 29), contributed to the formation of the early lesions (Fig. 3C). With time (30
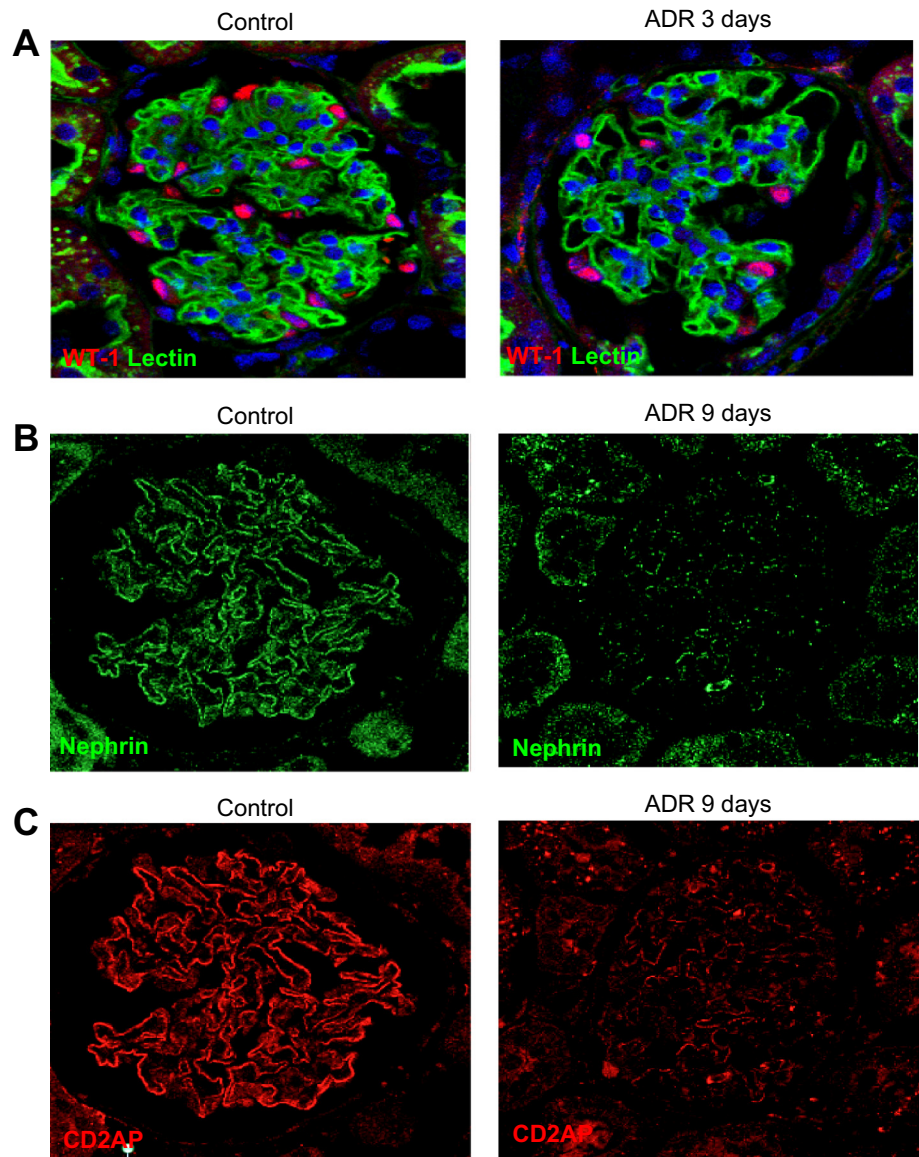
Fig. 2. Adriamycin (ADR) causes loss of podocytes and reduces the expression of the podocyte-associated proteins nephrin and CD2AP. *A*: representative micrographs of renal sections from control and ADR-treated rats showing triple labeling of a glomerulus for podocytes (WT-1-positive nuclei in red), for glomerular capillaries (lectin, green), and for cell nuclei (DAPI in blue). Nephrin (*B*) and CD2AP (*C*) expression in glomeruli from control and ADR rats. Representative micrographs are shown. Original magnification: ×400.

days), multilayers of cells accumulated at the site of synechiae resulting in more severe crescentic-like lesions (Fig. 3*A*).

A mild degree of glomerulosclerosis characterized by accumulation of the extracellular matrix material and obliteration of the capillary filter was observed 16 days after ADR, which became more evident at 30 days (glomerulosclerosis index, control rats: 0; ADR, *day 16*: 0.15 ± 0.06; *day 30*: 0.39 ± 0.09).

MSCs retention in the injured kidney of rats with ADR nephropathy. Because of the severity of the disease, an experimental protocol with repeated infusions of MSCs was applied to ADR-treated rats to maintain a constant number of MSCs in the kidney during the study. The ability of MSCs to reach the kidney in response to injury was assessed by prelabeling MSCs with PKH-26 fluorescent dye, before their in vivo injection. We found that the frequency of PKH-26-positive MSCs present in the kidney averaged 4.33 ± 0.38, 4.85 ± 0.43, and 5.73 ± 2.85 cells/100,000 renal cells, respectively, at *days 3*, *9*, and *16* after ADR, as assessed 15 h after MSC injection. Thirty-four percent of PKH-26-labeled MSCs were found in the glomeruli (Fig. 4*A*). Moreover, FACS analysis of dissoci-

ated renal tissue of ADR-treated rats receiving MSCs labeled with another tracer, rhodamine-B-conjugated nanoparticles, was also performed. Kidney samples of ADR rats receiving fluoNP-labeled MSCs showed 3.6 ± 0.2% positive cells for rhodamine B-fluoNP. The labeled MSCs localized in the glomeruli did not show positivity for the podocyte marker WT-1 (Fig. 4*B*).

Renal functional parameters in ADR rats receiving MSCs. Rats injected with a single dose of 5 mg/kg ADR exhibited proteinuria within 6 days (133 ± 8 vs. basal, 19 ± 1 mg/day; $P < 0.01$). Proteinuria progressively increased during time averaging 1,004 ± 33 mg/day at *day 30* in ADR rats given saline (Fig. 4*C*). The repeated infusions of MSCs did not affect the development of proteinuria at any time of the study.

In ADR rats given saline serum creatinine levels tended to increase during time compared with controls, although a statistical significance was not achieved (ADR, *day 9*: 0.60 ± 0.09; *day 16*: 0.73 ± 0.01; *day 30*: 0.86 ± 0.02 vs. controls: 0.58 ± 0.01 mg/dl). In ADR rats that received MSC therapy, serum creatinine levels were not different from those of rats
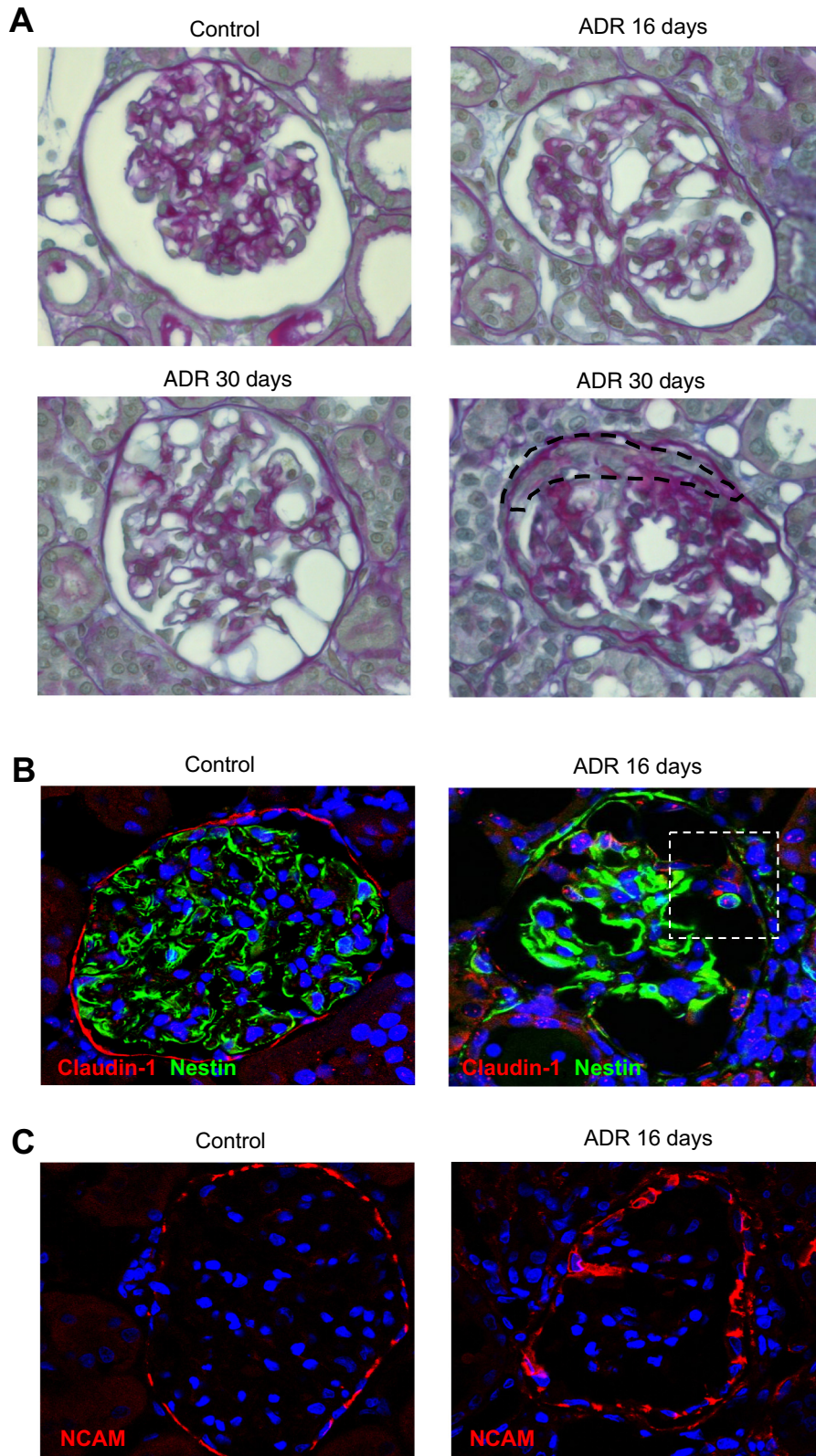
Fig. 3. Glomerular lesions in rats with ADR nephropathy at 16 and 30 days. *A*: representative micrographs of kidney tissue from control and ADR rats. Synechiae and more extensive adhesions or crescents-like lesions were observed during time in ADR-treated rats. Original magnification, ×400. *B*: representative images of claudin-1 (red) and nestin (green) in control and ADR rats. *Inset*: claudin-1- and nestin-positive cells that participated to the formation of early cellular bridge. Cells were costained with DAPI (blue). Original magnification: ×400. *C*: representative images of NCAM (red) in control and ADR rats. In ADR rats, NCAM$^+$ cells contributed to the formation of early lesions. Cells were costained with DAPI (blue). Original magnification: ×400.

given saline (ADR + MSCs, *day 16*: 0.80 ± 0.03; *day 30*: 0.81 ± 0.06 mg/dl).

MSC treatment preserves glomerular architecture. Treatment with MSCs limited early podocyte depletion, as indicated by the significantly ($P < 0.01$) higher number of podocytes per glomerulus at *day 3*, *9*, and *16* in the group of ADR-treated rats receiving MSCs compared with saline (Fig. 4D). The preservation of podocyte number was also confirmed by nestin
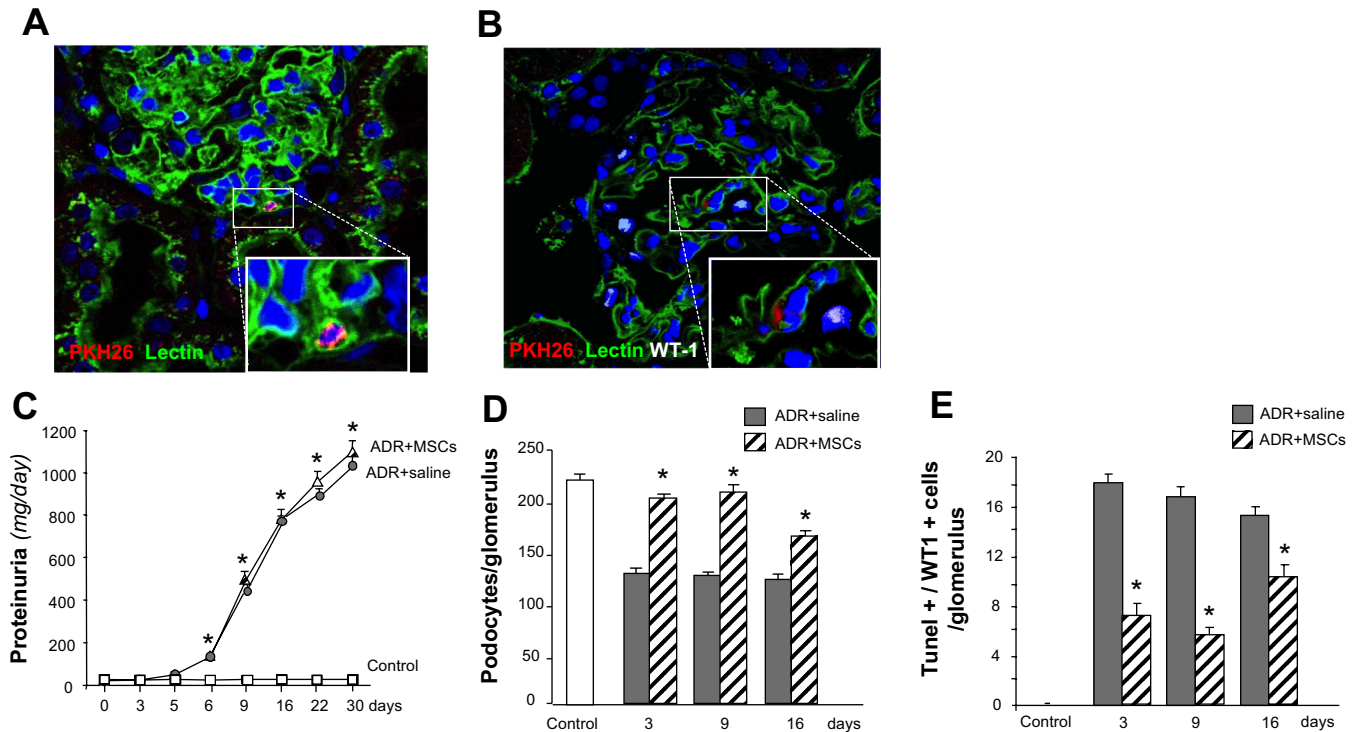
Fig. 4. *A*: representative micrographs of kidney tissue from ADR-treated rats injected with PKH26-labeled MSCs (red) at 3 days. Sections were costained with lectin wheat germ agglutinin (WGA; green) and DAPI (blue). Original magnification: × 400. *B*: representative micrograph of kidney sections of ADR-treated rats injected with PKH-26-labeled MSCs (red) stained with the podocyte marker WT1 (white) at 16 days. Sections were costained with lectin WGA (green) and DAPI (blue). Original magnification: ×400. *C*: time course of urinary protein excretion in control and ADR rats treated with saline or MSCs. Values are means ± SE. *$P < 0.01$ vs. control rats at corresponding time. *D*: morphometrical estimation of average number of podocytes per glomerulus from 3 to 16 days in ADR rats treated with saline or MSCs, and in control rats. Values are means ± SE. *$P < 0.01$ vs. ADR + saline at corresponding time. *E*: quantification of apoptotic podocytes, double positive for terminal deoxynucleotidyl transferase-mediated deoxyuridine triphosphate nick end-labeling (TUNEL) and WT-1 in glomeruli of ADR rats given saline or MSCs at *day 3*, *9*, and *16* and in control rats. Values are expressed as means ± SE. *$P < 0.01$ vs. ADR + saline at corresponding time.

expression (glomerular area percentage: ADR + MSCs, *day 3*: 18.19 ± 2.6%; $P < 0.01$ vs. ADR). The protective effect of MSC therapy against podocyte loss was associated with a partial, although significant, preservation of both nephrin and CD2AP expression compared with ADR rats given saline at *day 9* (nephrin, glomerular area percentage: ADR + MSCs, 3.81 ± 0.34%; $P < 0.05$ vs. saline; CD2AP, glomerular area percentage: ADR + MSCs, 5.24 ± 0.24%; $P < 0.05$ vs. saline).

MSCs displayed a marked antiapoptotic effect as indicated by the lower number ($P < 0.01$) of TUNEL-positive WT1-positive podocytes in renal tissue of MSC-treated rats with respect to ADR rats on saline at the corresponding times (Fig. 4*E*).

Consistent with the ability of infused MSCs to reduce podocyte dysfunction, stem cell treatment also significantly limited the presence of glomerular podocyte-PEC bridges. Specifically, in ADR rats receiving MSCs the percentage of glomeruli showing >50% adhesion of the tuft to the Bowman's capsule was significantly lower than that observed in rats given saline (Fig. 5*A*). In control animals, no glomeruli with adhesions >50% were found (Fig. 5*A*). Following MSC therapy, the distribution of NCAM-positive progenitor cells was restored along the Bowman's capsule to a pattern similar to controls (Fig. 5*B*). MSC treatment decreased the extension of sclerotic lesions at *day 30* as indicated by a significant ($P < 0.01$) reduction of the glomerulosclerosis index compared with ADR rats receiving saline (Fig. 5*C*).

MSCs increase glomerular VEGF level and limit endothelial cell damage. In search for factors possibly involved in MSC-mediated renoprotection in ADR rats, we focused on VEGF, highly produced by MSCs (13) and podocytes (16, 18, 46) and known to exert prosurvival and angiogenic activity (48, 50). As shown in Fig. 6*A*, VEGF staining was significantly ($P < 0.01$) reduced in glomeruli of ADR-treated rats compared with control rats. Infusions with MSCs enhanced glomerular VEGF expression, so that at *days 9* and *16* scores of VEGF expression in rats receiving MSCs were significantly higher than those of rats given saline. Consistently, Western blot experiments performed in renal tissue of all the experimental groups showed that at *days 9* and *16*, MSC treatment almost normalized renal levels of VEGF protein (Fig. 6*B*). Based on the evidence that VEGF is necessary for glomerular endothelial cell integrity and function (12, 46), next we evaluated whether high levels of glomerular VEGF in response to MSC infusion translated into preservation of glomerular endothelial cells. By morphometric analysis of the glomerular endothelium labeled with RECA, a marker of rat endothelial cells, we observed a marked reduction in volume density of endothelial cells in ADR-treated rats given saline compared with control rats (Fig. 6*C*). The degree of microvessel rarefaction was significantly limited in glomeruli of ADR rats infused with MSCs vs. glomeruli of nephrotic rats on saline.

Anti-inflammatory effect of MSCs. An increased number of ED1-positive monocytes/macrophages was found in the glom-
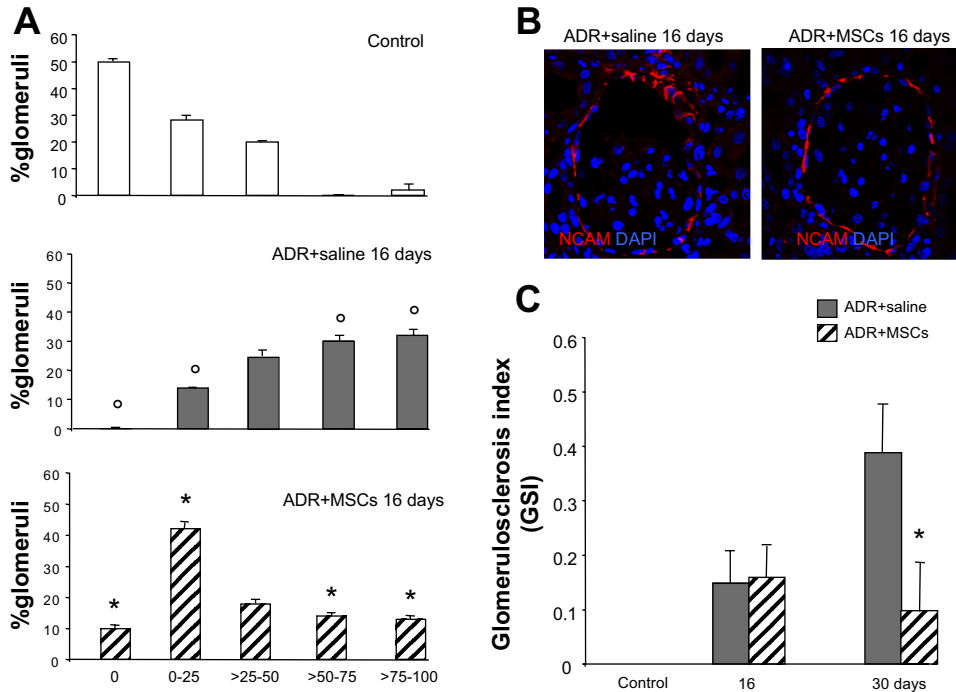
Fig. 5. MSCs preserve glomerular niches in ADR rats. *A*: percentage of glomeruli (means ± SE) affected by different degree of synechiae at 16 days in control and ADR rats receiving saline or MSCs. °*P* < 0.01 vs. control; **P* < 0.01 vs. ADR + saline. *B*: representative images of NCAM^{+} cells (red) in ADR rats receiving saline or MSCs at 16 days. Cells were costained with DAPI (blue). Original magnification: ×400. *C*: glomerulosclerosis index evaluated at 16 and 30 days in ADR rats receiving saline or MSCs, and in control rats. Original magnification: ×400. Score values are means ± SE. **P* < 0.01 vs. ADR + saline at corresponding time.

eruli of ADR-treated rats given saline compared with control rats (ADR, *day 9*: 4.31 ± 0.22; day 16: 4.78 ± 0.23 vs. control 1.11 ± 0.14 ED-1-positive cells/glomerulus; *P* < 0.05). Treatment with MSCs resulted in a marked anti-inflammatory effect as shown by a significant (*P* < 0.05) reduction of glomerular cell infiltrates with respect to ADR rats on saline (ADR + MSCs, *day 9*: 1.87 ± 0.06; *day 16*: 2.78 ± 0.31 ED-1-positive cells/glomerulus).

In Vitro Studies

MSCs protect podocytes from ADR-induced toxicity via VEGF. The capability of MSCs to exert protective effects on podocytes was investigated in coculture of MSCs with podocytes pretreated with ADR. Murine differentiated podocytes were exposed to ADR, and 72 h after drug withdrawal, cell count was performed. The number of viable podocytes was significantly (*P* < 0.01) reduced after ADR compared with control podocytes (Fig. 7*A*). Exposure of ADR-treated podocytes to murine MSCs completely prevented podocyte loss caused by ADR (*P* < 0.01; Fig. 7*A*). MSCs seeded alone did not proliferate. Since murine MSCs (20, 34) and podocytes (16, 18, 46) produce high levels of VEGF, we tested in the coculture system the contribution of VEGF in MSC-induced podocyte survival. Actually, blocking of VEGF with a specific antibody resulted in the abrogation of MSC protective effects on ADR-treated podocytes (Fig. 7*B*). Providing further evidence for a role of VEGF, we found that addition of exogenous VEGF to ADR-treated podocytes prevented cell loss at a similar extent as MSCs did (Fig. 7*B*).

To study whether MSCs could counteract podocyte apoptosis induced by ADR, we evaluated the expression of cytochrome *c*, a marker of intrinsic apoptosis when released from mitochondria into the cell cytosol (5, 26, 37). We found that ADR caused apoptosis in a high number of podocytes at 3, 15, and 24 h (*P* < 0.01 vs. control podocytes; Fig. 7, *C* and *D*).

When MSCs were cocultured with ADR-treated podocytes, a significant (*P* < 0.01) reduction of the percentage of apoptotic podocytes was found at all the considered times (Fig. 7, *C* and *D*). The protective effect exerted by MSCs was abrogated by the addition of a specific functional blocking anti-VEGF antibody to the coculture system (Fig. 7, *C* and *D*). The antiapoptotic activity of MSCs was further confirmed by evaluating cleaved caspase-3 in cells exposed to ADR at different times. ADR-treated podocytes exposed to MSCs showed a significant (*P* < 0.01) decrease in the percentage of cells positive for cleaved caspase-3 at 3 h (control podocytes: 4.7 ± 0.4; ADR: 15.3 ± 2.1; and ADR + MSCs: 6.0 ± 0.7% apoptotic cells) and at 15 h (ADR: 26.0 ± 1.0; and ADR + MSCs: 8.7 ± 1.1% apoptotic cells) in respect to ADR-treated podocytes exposed to medium alone. Exposure to VEGF markedly reduced the percentage of apoptotic cells in response to ADR at 3 h (10.5 ± 2.6%) and at 15 h (8.0 ± 1.4%; *P* < 0.01 vs. ADR).

The serine threonine kinase Akt is a critical factor in the regulation of prosurvival signals (9). Podocytes constitutively expressed the phosphorylated form of Akt, which was markedly reduced in podocytes damaged by ADR, as evaluated by Western blot analysis (Fig. 7*E*). Conditioned medium from MSCs markedly stimulated activation/phosphorylation of Akt in podocytes 72 h after ADR incubation (Fig. 7*E*). Addition of exogenous VEGF to ADR-pretreated podocytes increased phosphorylated-Akt protein expression at a similar level as MSC-conditioned medium (Fig. 7*E*).

DISCUSSION

The present study demonstrated for the first time that in rats with ADR-induced nephropathy, an established model of progressive glomerulosclerosis, glomerular podocyte injury preceded the activation of PECs, which participated together with podocytes to the formation of the synechiae followed by extensive adhesions between the Bowman's capsule and the
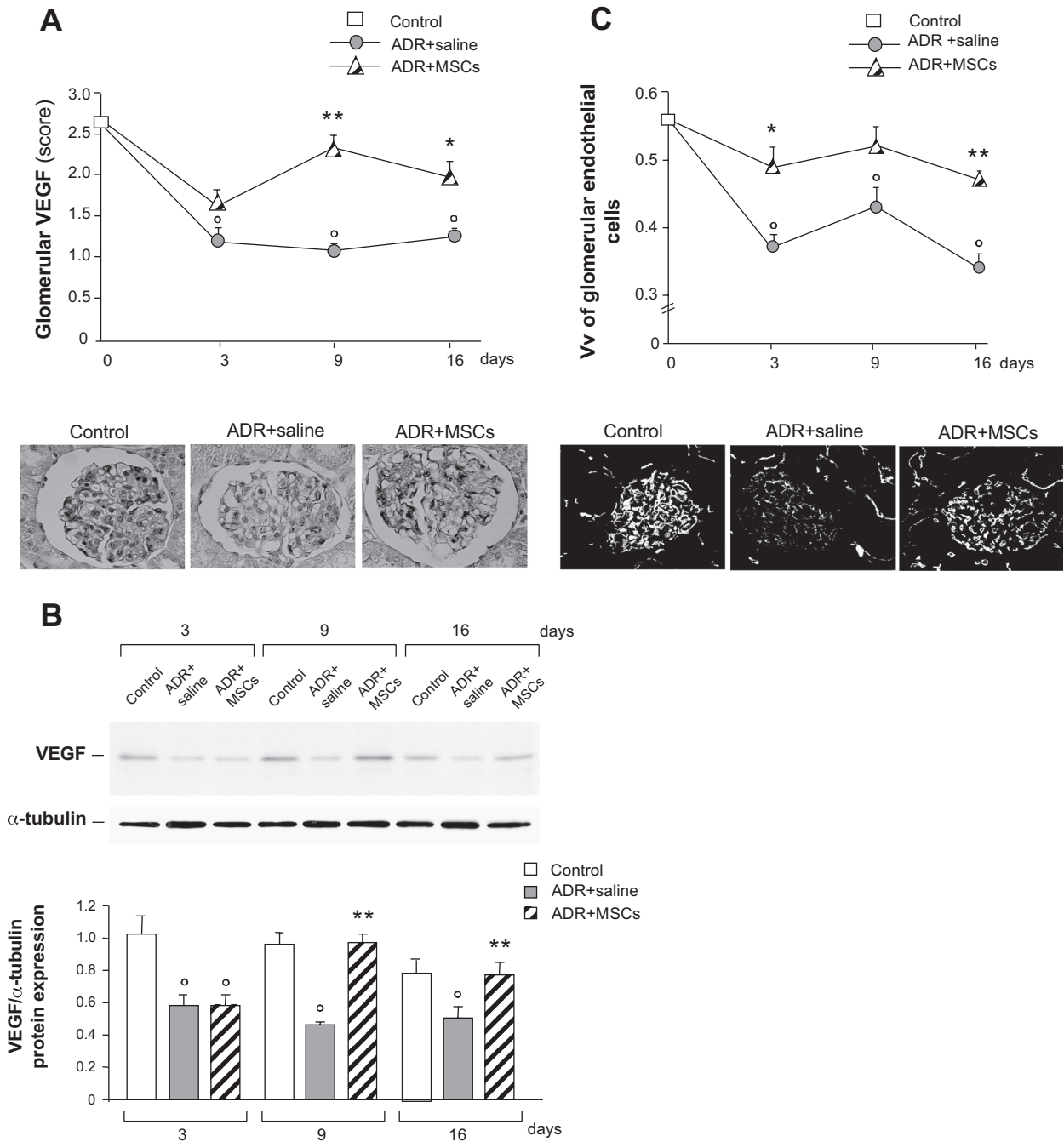
Fig. 6. Effect of MSC treatment on VEGF expression and volume density of glomerular endothelial cells in the kidney of ADR-treated rats. *A*: scores of glomerular VEGF expression evaluated at 3, 9, and 16 days after ADR in rats receiving saline or MSCs, or in control rats (*top*). Score values are means ± SE. °$P < 0.01$ vs. control; *$P < 0.05$, **$P < 0.01$ vs. ADR + saline at corresponding time. Representative micrographs at day 9 are shown (bottom). Original magnification: ×400. *B*: Western blot analysis of VEGF in kidney tissue of ADR rats receiving saline or MSCs, and control rats at 3, 9, 16 days (*top*). Expression levels of VEGF are quantified relative to levels of α-tubulin (*bottom*). Data are means ± SE.°$P < 0.01$ vs. control; **$P < 0.01$ vs. ADR + saline at corresponding time. *C*: estimation of volume density (Vv) of glomerular endothelial cells stained for RECA during time. Score values are means ± SE. °$P < 0.01$ vs. control; *$P < 0.05$, **$P < 0.01$ vs. ADR + saline at corresponding time. Representative micrographs at 16 days of glomerular RECA staining (*bottom*) in ADR rats receiving saline or MSCs and in control rats. Original magnification: × 400.

glomerular capillary loop. More importantly, claudin-positive PECs present at the adhesion sites expressed also the metanephric mesenchymal marker NCAM (1, 2, 29), indicating their progenitor nature. In human adult kidney, a hierarchical population of progenitors organized in a precise sequence along the Bowman's capsule has been identified that represents

a reservoir of cells contributing to the turnover of senesced or injured podocytes (39). However, in glomerular diseases in response to a severe podocyte damage an aberrant repair may take place, with an excessive proliferative response of renal progenitor cells from the Bowman's capsule, that contributes to hyperplastic lesions of podocytopathies and crescentic glo-
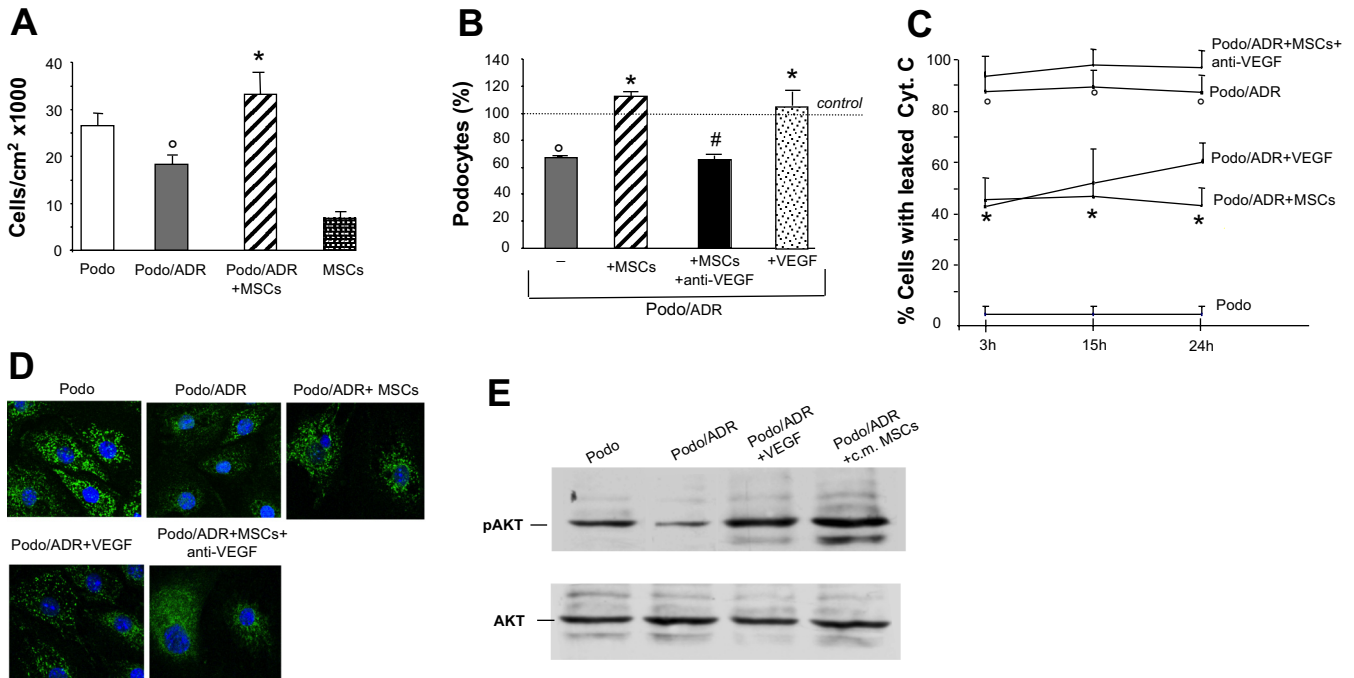
Fig. 7. MSCs exert protective effects on cultured ADR-treated podocytes via VEGF. *A*: MSCs protected podocytes from ADR-induced damage after 72 h of coculture. Podocytes were incubated with 1.5 µM ADR for 6 h, and after drug withdrawal, were cocultured with MSCs. After 72 h, viable cells were counted. Data are expressed as means ± SE. °$P < 0.01$ vs. Podo; *$P < 0.01$ vs. Podo/ADR. *B*: percentage of viable ADR-treated podocytes alone or cocultured with MSCs in the presence or absence of anti-VEGF antibody (10 µg/ml) for 72 h. In additional samples, ADR-treated podocytes were incubated with exogenous VEGF (40 ng /ml) for 72 h. Data (means ± SE) are expressed as percentage of viable podocytes in each sample vs. control podocytes imposed as 100%. °$P < 0.01$ vs. control; *$P < 0.01$ vs. Podo/ADR; #$P < 0.01$ vs. Podo/ADR + MSCs. *C*: effect of MSCs on podocyte apoptosis at different time intervals. ADR-treated podocytes alone or cocultured with MSCs in the presence or absence of functional blocking anti-VEGF antibody. In additional samples, ADR-treated podocytes were incubated with exogenous VEGF. Apoptosis was expressed as the percentage of podocytes with cytochrome *c* (Cyt C) released into cell cytosol. °$P < 0.01$ vs. Podo, *$P < 0.01$ vs. Podo/ADR. *D*: representative images of Cyt C expression (green) in podocytes 3 h after ADR incubation. Cyt C expression is also shown in ADR-treated podocytes cocultured with MSCs with or without anti-VEGF antibody, and in ADR-treated podocytes incubated with exogenous VEGF. Cells were costained with DAPI (blue). Original magnification: ×630. *E*: Western blot analysis of Akt at 72 h. Expression level of phosphorylated (p)-Akt Ser437 and total Akt was assessed in control podocytes exposed to medium (Podo), ADR-treated podocytes incubated with medium (Podo/ADR), VEGF (Podo/ADR+VEGF), or with MSC-conditioned medium (Podo/ADR + c.m. MSCs).

merulonephritis (25, 44). Using genetic tagging of either PECs or podocytes in experimental crescentic nephrotoxic nephritis, collapsing glomerulopathy, and FSGS models, it was shown that PECs represented the majority of cells that populated advanced cellular lesions (44, 45). We recently provided the evidence for the presence of renal progenitor cells within the Bowman's capsule of adult rat kidney by showing that the stemness markers NCAM and CD24 (8, 39) were expressed by the large majority of claudin1-positive PECs (3). In the MWF rat model characterized by spontaneous podocyte loss, extracapillary crescents and glomerulosclerosis, a high percentage of claudin-positive PECs expressing NCAM, and to a lesser extent WT1-positive podocytes, were found in hyperplastic lesions during disease progression, suggesting that renal injury in this model could be the consequence of progenitor cell dysfunction (3). We extended these observations to the rat model of ADR-induced podocyte injury where initial dysfunction of podocytes was followed by intercellular bridges between nestin-positive podocytes and claudin-positive PECs and by more extensive areas of adhesions between the Bowman's capsule and the tuft. The presence of NCAM-positive cells in such lesions implies that progenitor cells of parietal origin, in response to ADR-induced podocyte damage, acquired a migratory phenotype and invaded the glomerular tuft participating to the formation of crescents-like lesions and glomerular sclerosis.

Another unprecedented finding of the present study is that glomerular podocytes and progenitor cells represent critical cellular targets of MSC therapy in rats with ADR nephropathy. We showed that repeated MSC injections by exerting a remarkable antiapoptotic effect limited podocyte depletion and partially restored nephrin and CD2AP expression. The protective effect of MSCs against podocyte dysfunction and loss translated into less number of adhesions between PECs and podocytes, with the reestablishment of a normal localization of NCAM-positive PECs along the Bowman's capsule. Thus, stem cell therapy by reducing podocyte injury restored parietal progenitor cell regenerative capacity thereby ameliorating glomerular architecture and preventing sclerotic lesions. The fact that MSC treatment failed to reduce proteinuria in ADR rats could be abscribed to the limited recovery of the podocyte slit diaphragm proteins that were therefore unable to reestablish a normal function of foot processes.

Among factors possibly responsible of MSC-mediated glomerular protection in ADR rats, we studied VEGF, highly produced in vitro and in vivo by MSCs (13, 50), which critically regulates and maintains podocyte and glomerular endothelial cell integrity and function (12, 46). VEGF, abundantly produced also by podocytes (11, 12, 16), can promote glomerular endothelial cell repair (12, 23, 36) and activate prosurvival signals counteracting cell apoptosis (14). Studies

have documented that alterations in VEGF expression were associated with glomerular diseases (12, 23, 36). We found that treatment with MSCs recovered glomerular VEGF levels that were markedly reduced by ADR toxicity in rats given saline. Of note, high levels of VEGF were associated to a remarkable regenerative effect on glomerular capillary tuft in terms of a significant limitation of capillary rarefaction in ADR rats infused with MSCs. It is plausible to hypothesize that MSCs retained in the glomerulus could locally release VEGF that by promoting podocyte prosurvival programs would render podocytes again metabolically active to synthesize great amount of the proregenerative growth factor itself. That VEGF may exert a beneficial effect on podocytes is supported also by data showing that nephrin and CD2AP, target proteins regulated by VEGF (16, 18, 46), were partially preserved in renal tissue of MSC-treated animals.

The regenerative effect of MSC-derived VEGF on ADR-damaged podocytes was explored in coculture setting. In agreement with the in vivo data, MSCs significantly enhanced viability and limited apoptosis of podocytes in response to a toxic concentration of ADR. Such a prosurvival effect was markedly abrogated by a neutralizing anti-VEGF antibody, thereby indicating a cytoprotective action of VEGF on podocytes. The involvement of Akt, a key factor in the regulation of prosurvival signals, was documented by our finding of its activation/ phosphorylation in ADR-treated podocytes when exposed to MSC-conditioned medium or directly to exogenous VEGF. Similarly, previous studies (6, 14, 15) showed that VEGF induced the activation of Akt signaling pathway in several cell types, thus reducing apoptosis.

In summary, our data indicate that early podocyte injury and subsequent chaotic migration of parietal epithelial progenitor cells pave the way to crescents-like lesions and glomerulosclerosis in ADR nephropathy. Treatment with MSCs creates a glomerular pro-regenerative environment possibly by enhancing glomerular levels of VEGF, a factor able to activate Akt, a kinase upstream target of antiapoptotic and prosurvival pathways in podocytes. The restoration of podocyte number and function could limit migration and proliferation of parietal progenitor epithelial cells of the Bowman's capsule thereby reducing the early formation of PEC-podocyte bridges. These renoprotective effects were also accomplished by anti-inflammatory effects of MSC therapy that markedly reduced glomerular macrophage infiltration and local release of chemoattractants possibly involved in PEC-podocyte activation.

Strategies to enhance MSC retention in the kidney and renoprotection by preconditioning or genetic modifications could be helpful to enhance MSC local effect in the damaged kidneys thus improving also proteinuria and renal functional parameters.

AUTHOR CONTRIBUTIONS

Author contributions: C. Zoja, A.B., G.R., and M.M. conception and design of research; C. Zoja, P.B.G., C.R., S.C., E.G., D.C., C. Zanchi, P.B., and M.M. analyzed data; C. Zoja, P.B.G., C.R., S.C., E.G., D.C., C. Zanchi, P.B., A.B., G.R., and M.M. interpreted results of experiments; C. Zoja, P.B.G., S.C., E.G., D.C., and M.M. drafted manuscript; C. Zoja, C.R., A.B., G.R., and M.M. edited and revised manuscript; C. Zoja, P.B.G., C.R., S.C., E.G., D.C., C. Zanchi, P.B., A.B., G.R., and M.M. approved final version of manuscript; P.B.G., C.R., S.C., E.G., D.C., C. Zanchi, and P.B. performed experiments; C.R., S.C., E.G., D.C., and C. Zanchi prepared figures.

REFERENCES

1. **Abbate M, Brown D, Bonventre JV.** Expression of NCAM recapitulates tubulogenic development in kidneys recovering from acute ischemia. *Am J Physiol Renal Physiol* 277: F454–F463, 1999.
2. **Bard JB, Gordon A, Sharp L, Sellers WI.** Early nephron formation in the developing mouse kidney. *J Anat* 199: 385–392, 2001.
3. **Benigni A, Morigi M, Rizzo P, Gagliardini E, Rota C, Abbate M, Ghezzi S, Remuzzi A, Remuzzi G.** Inhibiting angiotensin-converting enzyme promotes renal repair by limiting progenitor cell proliferation and restoring the glomerular architecture. *Am J Pathol* 179: 628–638, 2011.
4. **Benigni A, Zoja C, Tomasoni S, Campana M, Corna D, Zanchi C, Gagliardini E, Garofano E, Rottoli D, Ito T, Remuzzi G.** Transcriptional regulation of nephrin gene by peroxisome proliferator-activated receptor-gamma agonist: molecular mechanism of the antiproteinuric effect of pioglitazone. *J Am Soc Nephrol* 17: 1624–1632, 2006.
5. **Brooks C, Wei Q, Cho SG, Dong Z.** Regulation of mitochondrial dynamics in acute kidney injury in cell culture and rodent models. *J Clin Invest* 119: 1275–1285, 2009.
6. **Cai J, Ahmad S, Jiang WG, Huang J, Kontos CD, Boulton M, Ahmed A.** Activation of vascular endothelial growth factor receptor-1 sustains angiogenesis and Bcl-2 expression via the phosphatidylinositol 3-kinase pathway in endothelial cells. *Diabetes* 52: 2959–2968, 2003.
7. **Cavaglieri RC, Martini D, Sogayar MC, Noronha IL.** Mesenchymal stem cells delivered at the subcapsule of the kidney ameliorate renal disease in the rat remnant kidney model. *Transplant Proc* 41: 947–951, 2009.
8. **Challen GA, Martinez G, Davis MJ, Taylor DF, Crowe M, Teasdale RD, Grimmond SM, Little MH.** Identifying the molecular phenotype of renal progenitor cells. *J Am Soc Nephrol* 15: 2344–2357, 2004.
9. **Datta SR, Brunet A, Greenberg ME.** Cellular survival: a play in three Akts. *Genes Dev* 13: 2905–2927, 1999.
10. **Davis BJ, Forbes JM, Thomas MC, Jerums G, Burns WC, Kawachi H, Allen TJ, Cooper ME.** Superior renoprotective effects of combination therapy with ACE and AGE inhibition in the diabetic spontaneously hypertensive rat. *Diabetologia* 47: 89–97, 2004.
11. **Eremina V, Cui S, Gerber H, Ferrara N, Haigh J, Nagy A, Ema M, Rossant J, Jothy S, Miner JH, Quaggin SE.** Vascular endothelial growth factor a signaling in the podocyte-endothelial compartment is required for mesangial cell migration and survival. *J Am Soc Nephrol* 17: 724–735, 2006.
12. **Eremina V, Sood M, Haigh J, Nagy A, Lajoie G, Ferrara N, Gerber HP, Kikkawa Y, Miner JH, Quaggin SE.** Glomerular-specific alterations of VEGF-A expression lead to distinct congenital and acquired renal diseases. *J Clin Invest* 111: 707–716, 2003.
13. **Figliuzzi M, Cornolti R, Perico N, Rota C, Morigi M, Remuzzi G, Remuzzi A, Benigni A.** Bone marrow-derived mesenchymal stem cells improve islet graft function in diabetic rats. *Transplant Proc* 41: 1797–1800, 2009.
14. **Foster RR, Saleem MA, Mathieson PW, Bates DO, Harper SJ.** Vascular endothelial growth factor and nephrin interact and reduce apoptosis in human podocytes. *Am J Physiol Renal Physiol* 288: F48–F57, 2005.
15. **Gerber HP, McMurtrey A, Kowalski J, Yan M, Keyt BA, Dixit V, Ferrara N.** Vascular endothelial growth factor regulates endothelial cell survival through the phosphatidylinositol 3'-kinase/Akt signal transduction pathway. Requirement for Flk-1/KDR activation. *J Biol Chem* 273: 30336–30343, 1998.
16. **Guan F, Villegas G, Teichman J, Mundel P, Tufro A.** Autocrine VEGF-A system in podocytes regulates podocin and its interaction with CD2AP. *Am J Physiol Renal Physiol* 291: F422–F428, 2006.

17. **Hallan SI, Coresh J, Astor BC, Asberg A, Powe NR, Romundstad S, Hallan HA, Lydersen S, Holmen J.** International comparison of the relationship of chronic kidney disease prevalence and ESRD risk. *J Am Soc Nephrol* 17: 2275–2284, 2006.

18. **Hara A, Wada T, Furuichi K, Sakai N, Kawachi H, Shimizu F, Shibuya M, Matsushima K, Yokoyama H, Egashira K, Kaneko S.** Blockade of VEGF accelerates proteinuria, via decrease in nephrin production in rat crescentic glomerulonephritis. *Kidney Int* 69: 1986–1995, 2006.

19. **Herrera MB, Bussolati B, Bruno S, Fonsato V, Romanazzi GM, Camussi G.** Mesenchymal stem cells contribute to the renal repair of acute tubular epithelial injury. *Int J Mol Med* 14: 1035–1041, 2004.

20. **Herrmann JL, Weil BR, Abarbanell AM, Wang Y, Poynter JA, Manukyan MC, Meldrum DR.** IL-6 and TGF-alpha costimulate mesenchymal stem cell vascular endothelial growth factor production by ERK-, JNK-, and PI3K-mediated mechanisms. *Shock* 35: 512–516, 2011.

21. **Imberti B, Morigi M, Tomasoni S, Rota C, Corna D, Longaretti L, Rottoli D, Valsecchi F, Benigni A, Wang J, Abbate M, Zoja C, Remuzzi G.** Insulin-like growth factor-1 sustains stem cell mediated renal repair. *J Am Soc Nephrol* 18: 2921–2928, 2007.

22. **Just PM, Riella MC, Tschosik EA, Noe LL, Bhattacharyya SK, de Charro F.** Economic evaluations of dialysis treatment modalities. *Health Policy* 86: 163–180, 2008.

23. **Kim YG, Suga SI, Kang DH, Jefferson JA, Mazzali M, Gordon KL, Matsui K, Breiteneder-Geleff S, Shankland SJ, Hughes J, Kerjaschki D, Schreiner GF, Johnson RJ.** Vascular endothelial growth factor accelerates renal recovery in experimental thrombotic microangiopathy. *Kidney Int* 58: 2390–2399, 2000.

24. **Laflamme MA, Murry CE.** Regenerating the heart. *Nat Biotechnol* 23: 845–856, 2005.

25. **Lasagni L, Romagnani P.** Glomerular epithelial stem cells: the good, the bad, and the ugly. *J Am Soc Nephrol* 21: 1612–1619, 2010.

26. **Lebrecht D, Setzer B, Rohrbach R, Walker UA.** Mitochondrial DNA and its respiratory chain products are defective in doxorubicin nephrosis. *Nephrol Dial Transplant* 19: 329–336, 2004.

27. **Macconi D, Bonomelli M, Benigni A, Plati T, Sangalli F, Longaretti L, Conti S, Kawachi H, Hill P, Remuzzi G, Remuzzi A.** Pathophysiologic implications of reduced podocyte number in a rat model of progressive glomerular injury. *Am J Pathol* 168: 42–54, 2006.

28. **Magnasco A, Corselli M, Bertelli R, Ibatici A, Peresi M, Gaggero G, Cappiello V, Chiavarina B, Mattioli G, Gusmano R, Ravetti JL, Frassoni F, Ghiggeri GM.** Mesenchymal stem cells protective effect in adriamycin model of nephropathy. *Cell Transplant* 17: 1157–1167, 2008.

29. **Metsuyanim S, Harari-Steinberg O, Buzhor E, Omer D, Pode-Shakked N, Ben-Hur H, Halperin R, Schneider D, Dekel B.** Expression of stem cell markers in the human fetal kidney. *PLos One* 4: e6709, 2009.

30. **Morigi M, Imberti B, Zoja C, Corna D, Tomasoni S, Abbate M, Rottoli D, Angioletti S, Benigni A, Perico N, Alison M, Remuzzi G.** Mesenchymal stem cells are renotropic, helping to repair the kidney and improve function in acute renal failure. *J Am Soc Nephrol* 15: 1794–1804, 2004.

31. **Morigi M, Introna M, Imberti B, Corna D, Abbate M, Rota C, Rottoli D, Benigni A, Perico N, Zoja C, Rambaldi A, Remuzzi A, Remuzzi G.** Human bone marrow mesenchymal stem cells accelerate recovery of acute renal injury and prolong survival in mice. *Stem Cells* 26: 2075–2082, 2008.

32. **Mundel P, Reiser J, Zuniga Mejia Borja A, Pavenstadt H, Davidson GR, Kriz W, Zeller R.** Rearrangements of the cytoskeleton and cell contacts induce process formation during differentiation of conditionally immortalized mouse podocyte cell lines. *Exp Cell Res* 236: 248–258, 1997.

33. **Nagaya N, Fujii T, Iwase T, Ohgushi H, Itoh T, Uematsu M, Yamagishi M, Mori H, Kangawa K, Kitamura S.** Intravenous administration of mesenchymal stem cells improves cardiac function in rats with acute myocardial infarction through angiogenesis and myogenesis. *Am J Physiol Heart Circ Physiol* 287: H2670–H2676, 2004.

34. **Ninichuk V, Gross O, Segerer S, Hoffmann R, Radomska E, Buchstaller A, Huss R, Akis N, Schlondorff D, Anders HJ.** Multipotent mesenchymal stem cells reduce interstitial fibrosis but do not delay progression of chronic kidney disease in collagen4A3-deficient mice. *Kidney Int* 70: 121–129, 2006.

35. **Ohse T, Pippin JW, Vaughan MR, Brinkkoetter PT, Krofft RD, Shankland SJ.** Establishment of conditionally immortalized mouse glomerular parietal epithelial cells in culture. *J Am Soc Nephrol* 19: 1879–1890, 2008.

36. **Ostendorf T, Kunter U, Eitner F, Loos A, Regele H, Kerjaschki D, Henninger DD, Janjic N, Floege J.** VEGF(165) mediates glomerular endothelial repair. *J Clin Invest* 104: 913–923, 1999.

37. **Park MS, De Leon M, Devarajan P.** Cisplatin induces apoptosis in LLC-PK1 cells via activation of mitochondrial pathways. *J Am Soc Nephrol* 13: 858–865, 2002.

38. **Perry J, Ho M, Viero S, Zheng K, Jacobs R, Thorner PS.** The intermediate filament nestin is highly expressed in normal human podocytes and podocytes in glomerular disease. *Pediatr Dev Pathol* 10: 369–382, 2007.

39. **Ronconi E, Sagrinati C, Angelotti ML, Lazzeri E, Mazzinghi B, Ballerini L, Parente E, Becherucci F, Gacci M, Carini M, Maggi E, Serio M, Vannelli GB, Lasagni L, Romagnani S, Romagnani P.** Regeneration of glomerular podocytes by human renal progenitors. *J Am Soc Nephrol* 20: 322–332, 2009.

40. **Sagrinati C, Netti GS, Mazzinghi B, Lazzeri E, Liotta F, Frosali F, Ronconi E, Meini C, Gacci M, Squecco R, Carini M, Gesualdo L, Francini F, Maggi E, Annunziato F, Lasagni L, Serio M, Romagnani S, Romagnani P.** Isolation and characterization of multipotent progenitor cells from the Bowman's capsule of adult human kidneys. *J Am Soc Nephrol* 17: 2443–2456, 2006.

41. **Semedo P, Correa-Costa M, Antonio Cenedeze M, Maria Avancini Costa Malheiros D, Antonia dos Reis M, Shimizu MH, Seguro AC, Pacheco-Silva A, Saraiva Camara NO.** Mesenchymal stem cells attenuate renal fibrosis through immune modulation and remodeling properties in a rat remnant kidney model. *Stem Cells* 27: 3063–3073, 2009.

42. **Shankland SJ.** The podocyte's response to injury: role in proteinuria and glomerulosclerosis. *Kidney Int* 69: 2131–2147, 2006.

43. **Shih NY, Li J, Cotran R, Mundel P, Miner JH, Shaw AS.** CD2AP localizes to the slit diaphragm and binds to nephrin via a novel C-terminal domain. *Am J Pathol* 159: 2303–2308, 2001.

44. **Smeets B, Angelotti ML, Rizzo P, Dijkman H, Lazzeri E, Mooren F, Ballerini L, Parente E, Sagrinati C, Mazzinghi B, Ronconi E, Becherucci F, Benigni A, Steenbergen E, Lasagni L, Remuzzi G, Wetzels J, Romagnani P.** Renal Progenitor Cells Contribute to Hyperplastic Lesions of Podocytopathies and Crescentic Glomerulonephritis. *J Am Soc Nephrol* 20: 2593–2603, 2009.

45. **Smeets B, Kuppe C, Sicking EM, Fuss A, Jirak P, van Kuppevelt TH, Endlich K, Wetzels JF, Grone HJ, Floege J, Moeller MJ.** Parietal epithelial cells participate in the formation of sclerotic lesions in focal segmental glomerulosclerosis. *J Am Soc Nephrol* 22: 1262–1274, 2011.

46. **Sugimoto H, Hamano Y, Charytan D, Cosgrove D, Kieran M, Sudhakar A, Kalluri R.** Neutralization of circulating vascular endothelial growth factor (VEGF) by anti-VEGF antibodies and soluble VEGF receptor 1 (sFlt-1) induces proteinuria. *J Biol Chem* 278: 12605–12608, 2003.

47. **Tang J, Xie Q, Pan G, Wang J, Wang M.** Mesenchymal stem cells participate in angiogenesis and improve heart function in rat model of myocardial ischemia with reperfusion. *Eur J Cardiothorac Surg* 30: 353–361, 2006.

48. **Togel F, Cohen A, Zhang P, Yang Y, Hu Z, Westenfelder C.** Autologous and allogeneic marrow stromal cells are safe and effective for the treatment of acute kidney injury. *Stem Cells Dev* 18: 475–485, 2009.

49. **Togel F, Hu Z, Weiss K, Isaac J, Lange C, Westenfelder C.** Administered mesenchymal stem cells protect against ischemic acute renal failure through differentiation-independent mechanisms. *Am J Physiol Renal Physiol* 289: F31–F42, 2005.

50. **Togel F, Weiss K, Yang Y, Hu Z, Zhang P, Westenfelder C.** Vasculotropic, paracrine actions of infused mesenchymal stem cells are important to the recovery from acute kidney injury. *Am J Physiol Renal Physiol* 292: F1626–F1635, 2007.

51. **Torrente Y, Polli E.** Mesenchymal stem cell transplantation for neurodegenerative diseases. *Cell Transplant* 17: 1103–1113, 2008.

52. **Tryggvason K, Wartiovaara J.** Molecular basis of glomerular permselectivity. *Curr Opin Nephrol Hypertens* 10: 543–549, 2001.

53. **Weibel E.** *Stereological Methods: Practical Methods for Morphometry.* New York: Academic 1979.

54. **Wiggins RC.** The spectrum of podocytopathies: a unifying view of glomerular diseases. *Kidney Int* 71: 1205–1214, 2007.

55. **Zoja C, Abbate M, Corna D, Capitanio M, Donadelli R, Bruzzi I, Oldroyd S, Benigni A, Remuzzi G.** Pharmacologic control of angiotensin II ameliorates renal disease while reducing renal TGF-beta in experimental mesangioproliferative glomerulonephritis. *Am J Kidney Dis* 31: 453–463, 1998.